nature
structural biology

© 2003 Nature Publishing Group http://www.nature.com/naturestructuralbiology

Pulling geometry defines the mechanical resistance of a β-sheet protein

David J Brockwell[1], Emanuele Paci[2], Rebecca C Zinober[1,3], Godfrey S Beddard[4], Peter D Olmsted[3], D Alastair Smith[3], Richard N Perham[5] & Sheena E Radford[1]

Proteins show diverse responses when placed under mechanical stress. The molecular origins of their differing mechanical resistance are still unclear, although the orientation of secondary structural elements relative to the applied force vector is thought to have an important function. Here, by using a method of protein immobilization that allows force to be applied to the same all-β protein, E2lip3, in two different directions, we show that the energy landscape for mechanical unfolding is markedly anisotropic. These results, in combination with molecular dynamics (MD) simulations, reveal that the unfolding pathway depends on the pulling geometry and is associated with unfolding forces that differ by an order of magnitude. Thus, the mechanical resistance of a protein is not dictated solely by amino acid sequence, topology or unfolding rate constant, but depends critically on the direction of the applied extension.

Experiments in which proteins are mechanically unfolded using an atomic force microscope (AFM) have shown that different proteins, even those with related structures, show a broad range of mechanical responses that are difficult to rationalize. For example, the I27 domain from titin unfolds at 200 pN at 600 nm s^{-1} (ref. 1). By contrast, fibronectin type III domains (FnIII), which have a similar immunoglobulin-like structure, unfold at forces that vary from 75 to 220 pN (at 600 nm s^{-1}) (ref. 2). It has been proposed, based upon both experimental[3] and theoretical[4,5] results, that the mechanical phenotypes of proteins may arise from differences in their topology, possibly as a result of variations in the number and position of hydrogen bonds among strands and sheets, and relative to the direction in which the force is applied. However, direct determination of the effect of extension geometry upon mechanical resistance is difficult to assess because, as well as having distinct topologies, different protein domains also vary in sequence and kinetic and thermodynamic stability.

Direct determination of the effect of pulling geometry on mechanical resistance thus requires that the same domain be studied. This ensures that other features that have been predicted to be important in determining a protein's mechanical resistance, such as amino acid sequence, the number and location of hydrogen bonds, the intrinsic unfolding rate constant and hydrophobic packing in the core, remain constant[4,5,6–9]. Here we present experiments that allow examination of the influence of pulling trajectory on the mechanical unfolding properties of a single protein domain. This was achieved with an approach in which the innermost lipoyl domain of the dihydrolipoyl acetyltransferase subunit (E2p) of the pyruvate dehydrogenase (PDH) multienzyme complex from *Escherichia coli* (E2lip3) was immobilized at different points to a gold substrate (**Fig. 1a**).

RESULTS

E2lip3 can be pulled in different directions

The three homologous lipoyl domains of *E. coli* E2p each consist of two four-stranded β-sheets, arranged as a flattened β-barrel[10,11] (**Fig. 1b**). The domains are post-translationally modified *in vivo* by attachment of lipoic acid specifically to the N6-amino group of a lysine residue, identified as Lys41 in E2lip3 (**Fig. 1b**). Lipoylated E2lip3, denoted here as E2lip3(+), has the dithiolane moiety of its lipoyl group located at the end of a mobile swinging arm capable of spanning 30 Å (ref. 10). Similarly to I27, the N- and C-terminal β-strands of E2lip3 are directly hydrogen bonded (**Fig. 1c,d**). Unlike I27, however, these strands are arranged in an antiparallel orientation.

To establish the mechanical unfolding properties of E2lip3, the protein was placed as the C-terminal module in an I27 scaffold (**Fig. 1a**). The parent $(I27)_5$ homopolymer has been described and is composed of five copies of a mutated C475 C635 domain[7,12]. $(I27)_5$ contains two C-terminal cysteine residues that permit immobilization of the concatamer onto a gold surface[13] (**Fig. 1a**). Extension of the concatamer under force then subjects each mutant I27 domain to a longitudinal shearing force. In a second concatamer $(I27)_4$E2lip3(+), the fifth domain is substituted with E2lip3 lipoylated at Lys41. This modification has no effect on the structure[11] or stability of the lipoyl domain (see Methods) but permits immobilization of the concatamer to the gold substrate by means of the dithiolane ring. As a consequence, a perturbation akin to a longitudinal shear is applied to the protein

[1]School of Biochemistry and Molecular Biology, University of Leeds, LS2 9JT, UK. [2]Biochemisches Institut der Univerität Zürich, Winterthurerstrasse 190, CH-8057 Zürich, Switzerland. [3]Department of Physics and Astronomy and [4]School of Chemistry, University of Leeds, Leeds LS2 9JT, UK. [5]Department of Biochemistry, University of Cambridge, Cambridge CB2 1GA, UK. Correspondence should be addressed to S.E.R. (S.E.Radford@leeds.ac.uk).

Published online 17 August 2003; doi:10.1038/nsb968

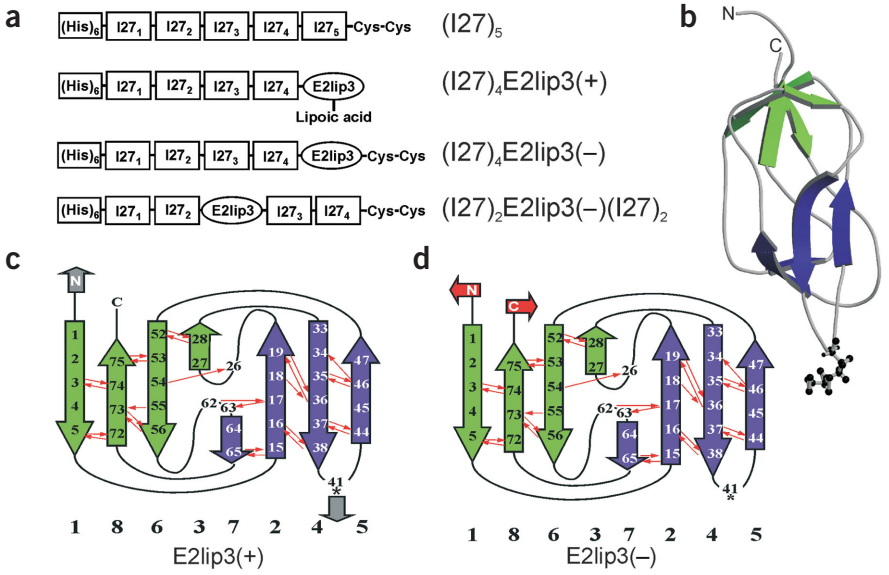

Figure 1 Structure of E2lip3 and its inclusion in concatamers of I27. (**a**) Schematic diagram of $(I27)_5$, $(I27)_4$E2lip3(+), $(I27)_4$E2lip3(–) and $(I27)_2$E2lip3(–)$(I27)_2$, $(I27)_5$, $(I27)_4$E2lip3(–) and $(I27)_2$E2lip3(–)$(I27)_2$ do not contain lipoic acid and are immobilized onto a gold surface by the two C-terminal cysteine residues. $(I27)_4$E2lip3(+) is immobilized via the dithiolane group of lipoic acid. Wild-type E2lip3 contains no cysteine. (**b**) Structure of E2lip3. The figure was drawn using MolScript[41] and Raster3D[42] using the coordinates 1QJO (ref. 10). The β-strands in each β-sheet are purple and green. Lys41 is shown as ball and stick. (**c**,**d**) Topology diagrams showing points of extension for E2lip3(+) and E2lip3(–), respectively. Residues involved in elements of secondary structure or forming hydrogen bonds (thin red arrows) are shown. Lipoylation of E2lip3(+) occurs at residue 41 (*). This residue is not lipoylated in E2lip3(–). Secondary structure elements and hydrogen bonds (>0.5 kcal mol^{-1}) were assigned using DSSP[43]. The β-strands are numbered 1–8, starting from the N-terminal strand.

during mechanical unfolding, although the precise manner in which force is applied to the protein is more complex than that for I27, because the β-strands containing the attachment points are not directly hydrogen bonded (denoted here as a shearlike extension). In the third construct $(I27)_4$E2lip3(–), the fifth I27 domain is replaced with an unlipoylated E2lip3 domain (E2lip3(–)), and in $(I27)_2$E2lip3(–)$(I27)_2$ the third domain is replaced with E2lip3(–). These constructs retain the two C-terminal cysteine residues (**Fig. 1a**). Mechanical unfolding of these constructs subjects E2lip3(–) to a force orthogonal to the β-strands, which has the effect of peeling them apart. Attachment of E2lip3 to the gold surface, through cysteines or lipoic acid, thus permits one to investigate the influence of pulling geometry on the mechanical unfolding properties of a protein domain so that the unfolding energy landscape can be explored in greater detail.

E2lip3(+) unfolds at a high force

Mechanical unfolding of $(I27)_5$ results in five peaks, each corresponding to the unfolding of an I27 domain, followed by a large tip-protein detachment event (**Fig. 2**). By repeating many approach-retract cycles (**Fig. 3a**, top) and constructing force- and distance-frequency histograms (**Fig. 3b**,**c**, top) $(I27)_5$ was found to unfold at 182 ± 5 pN (700 nm s^{-1}) and to produce an increase in length upon unfolding (measured by the interpeak distance L_i) of 24.0 ± 0.1 nm, in agreement with published values[7,12]. By fitting the rising edge of each peak to a simplified worm-like chain (WLC) model[14], a mean difference in contour length (ΔL_c) of 26.5 ± 0.2 nm was calculated, in accord with previous results[1,7,15].

The force-extension profile for $(I27)_4$E2lip3(+) also contains five unfolding events (**Fig. 2b**). One event, however, generates a shorter interpeak distance (L_i = 10.0 ± 0.2 nm) than that observed for the other four events (L_i = 24.2 ± 0.3 nm) (**Fig. 3a**,**c**, middle). Only one peak with L_i ~ 10 nm was observed in each trace, suggesting that this event (labeled * in **Fig. 2b**) represents the unfolding of E2lip3(+). The shorter chain length generated when E2lip3 unfolds, relative to that for I27, results in a higher restoring force being applied on the cantilever. Therefore, when this domain unfolds, the force returns to a higher value than expected and observed for an I27 domain unfolding at the same event number. The most frequently occurring event gives a ΔL_c (26.7 ± 0.2 nm), identical to that obtained for I27. The ΔL_c for the population with the shorter unfolding distance is 10.9 ± 0.2 nm, consistent with that expected (10 nm) for the unfolding of E2lip3(+) attached to gold via the lipoyl group at residue 41. The difference in ΔL_c between I27 and E2lip3 immobilized at Lys41 allows the unfolding forces for each domain type to be assigned unambiguously. The resultant force-frequency histogram (**Fig. 3b**, middle) shows that E2lip3 is highly resistant to extension (177 ± 3 pN at 700 nm s^{-1}) when extended from its N terminus and Lys41 (shearlike force). Notably, the unfolding forces for I27 in $(I27)_4$E2lip3(+) are significantly higher (ΔF = 10 pN at 700 nm s^{-1}) than those observed for this domain in $(I27)_5$, $(I27)_4$E2lip3(–) and $(I27)_2$E2lip3(–)$(I27)_2$ (**Fig. 4**). This effect arises from the faster loading rate applied onto the remaining I27 domains, because of the shorter length of polypeptide chain released when

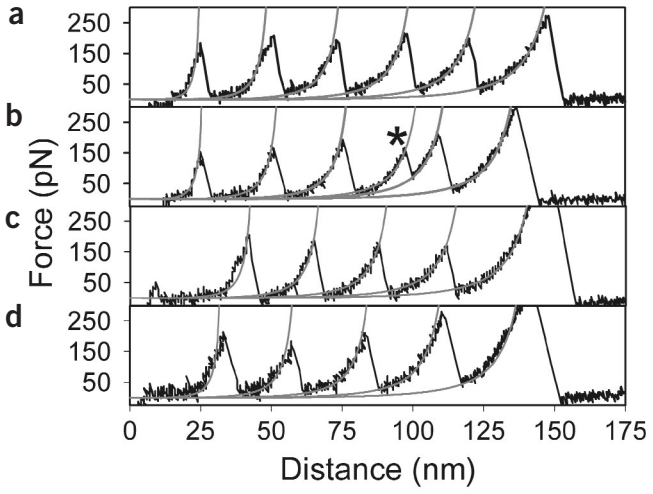

Figure 2 Force-extension curves of different concatamers. (**a**) $(I27)_5$. (**b**) $(I27)_4$E2lip3(+) (unfolding of E2lip3 is marked *). (**c**) $(I27)_4$E2lip3(–). (**d**) $(I27)_2$E2lip3(–)$(I27)_2$. The leading edge of each peak has been fitted to a simplified WLC model (gray line)[14] with a persistence length of 0.4 nm.

© 2003 Nature Publishing Group http://www.nature.com/naturestructuralbiology

© 2003 Nature Publishing Group http://www.nature.com/naturestructuralbiology

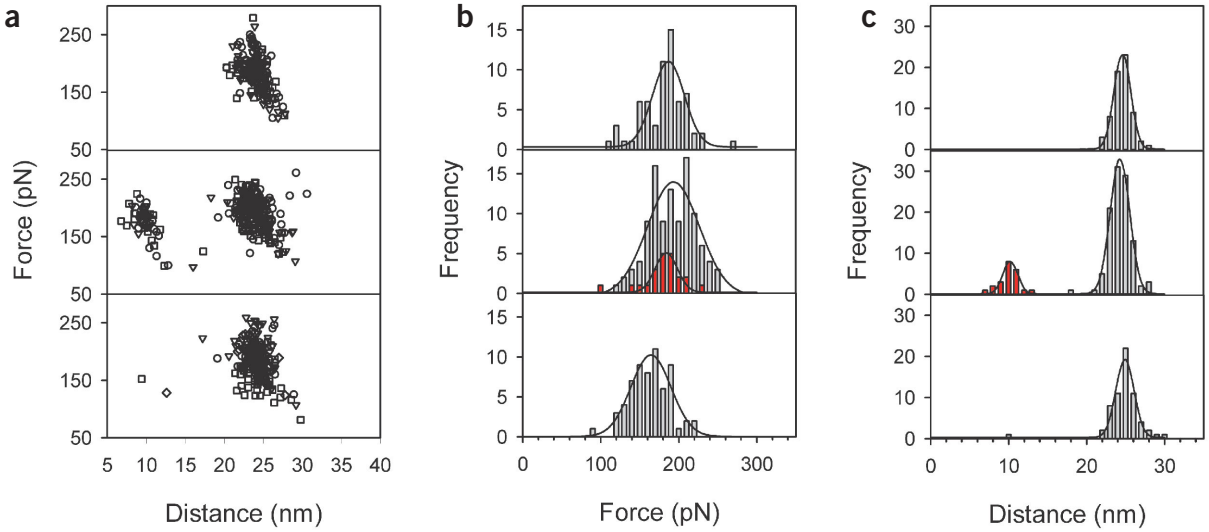

Figure 3 Mechanical unfolding statistics of $(I27)_5$, $(I27)_4$E2lip3(+) and $(I27)_4$E2lip3(–) at a tip-retraction speed of 700 nm s^{-1}. (**a**) Force-distance scattergrams of $(I27)_5$ (top), $(I27)_4$E2lip3(+) (middle) and $(I27)_4$E2lip3(–) (bottom), showing all peaks in all data sets (n = 70, 65, 45; n = 84, 71, 128; n = 57, 46, 63, 25, respectively). Different symbols represent each data set. (**b**,**c**) Force-frequency and distance-frequency histograms, respectively, for one experiment for $(I27)_5$ (n = 65) (top), $(I27)_4$E2lip3(+) (n = 128) (middle) and $(I27)_4$E2lip3(–) (n = 63) (bottom). Gray bars, forces and distances for I27; red bars, forces and distances for E2lip3(+). The distributions in each histogram were fitted to a simple four-parameter Gaussian (solid lines).

E2lip3(+), immobilized at residue 41, unfolds[12]. The magnitude of this effect observed experimentally is entirely consistent with Monte Carlo simulations of the unfolding of $(I27)_4$E2lip3(+) using parameters for C47S C63S I27 obtained earlier (see Methods and **Fig. 4**)[7].

What is the mechanical unfolding rate constant for E2lip3(+)?

E2lip3(+) is observed to unfold at any position in the unfolding sequence of $(I27)_4$E2lip3(+), ranging from the first (**Fig. 5a**, bottom trace) to the last unfolding peak (**Fig. 5a**, top trace). Mechanical unfolding is a kinetically controlled process[1,16]. The probabilistic nature of barrier crossing means that, in a heteropolymer, there is an interplay between the intrinsic unfolding rate constants at zero force (k_u^0), the number of each domain type and the distribution of observed unfolding forces[12]. For a concatamer composed of two domain types, therefore, it is possible to estimate the k_u^0 for the second domain type if one knows the composition of the copolymer as well as k_u^0 for the first domain type (see Methods). Fitting the analytical solution to the experimental probability of E2lip3(+) unfolding at each event number revealed that $k_u^0{}_{\mathrm{E2lip3(+)}} = 3.8 k_u^0{}_{\mathrm{I27}}$ (**Fig. 5b**). This approach was validated by simulating the unfolding process of $(I27)_4$E2lip3(+) using a Monte Carlo method[12]. The resultant force-extension profiles (**Fig. 5c**) show the same event number unfolding probability as was observed experimentally and predicted by theory (**Fig. 5b**). The validity of these results was tested further by comparison of the pulling-speed dependence of the unfolding forces for both domain types in $(I27)_4$E2lip3(+) measured experimentally with that generated by a Monte Carlo simulation using $k_u^0{}_{\mathrm{E2lip3(+)}} = 3.8 k_u^0{}_{\mathrm{I27}}$ (**Fig. 4**). The simulated-speed dependence of I27 (dashed line) and E2lip3(+) (solid line) show that the derived parameters predict the data well.

These data demonstrate, therefore, that when E2lip3(+) is subjected to a shearlike force, its mechanical unfolding properties, expressed in terms of k_u^0 and x_u (the distance from the native state to the transition state) are similar to those of I27. Therefore, when force is applied in a similar geometry to these disparate proteins that have different sequences, structures and function, they show similar mechanical unfolding behavior. This observation suggests that the orientation of the points of extension relative to the long axis of β-strands is an important determinant of the mechanical resistance of a protein.

$(I27)_4$E2lip3(–) unfolds at a very low force

The pulling geometry applied to E2lip3 was altered by immobilizing $(I27)_4$E2lip3(–) at its C terminus via two cysteine residues (**Fig. 1a**). Unlike the other constructs described earlier, only four unfolding

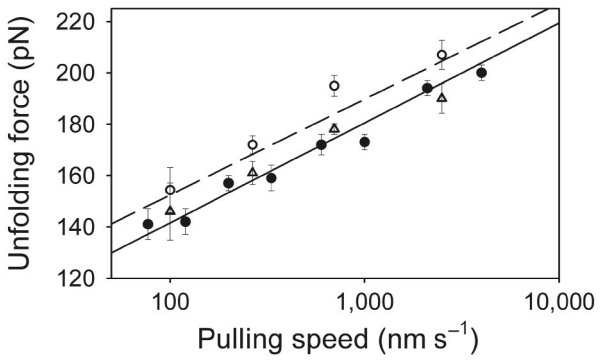

Figure 4 Pulling-speed dependence of unfolding forces for $(I27)_4$E2lip3(+) and $(I27)_5$* (a heteropolymer of I27 domains studied previously[7]). The mean unfolding force of triplicate data sets (± s.e.m.) at 100, 266, 700 and 2,500 nm s^{-1} for I27 (○) and E2lip3 (△) in $(I27)_4$E2lip3(+). The speed dependence for $(I27)_5$* (ref. 7) is shown for comparison (●). Continuous and discontinuous lines show the speed dependence of mechanical unfolding predicted for E2lip3(+) and I27 in $(I27)_4$E2lip3(+), that is, four domains of I27 and one of E2lip3(+) using a Monte Carlo simulation. Both the mean unfolding force and the speed dependence of the unfolding force for E2lip3(+) are experimentally indistinguishable from those obtained for $(I27)_5$* (ref. 7), even though E2lip3(+) would be expected to unfold at a lower force than I27 if each domain was concatamerized into homopolymers of identical length. This results from the number and length of previously unfolded domains that markedly affect the observed unfolding force[12].

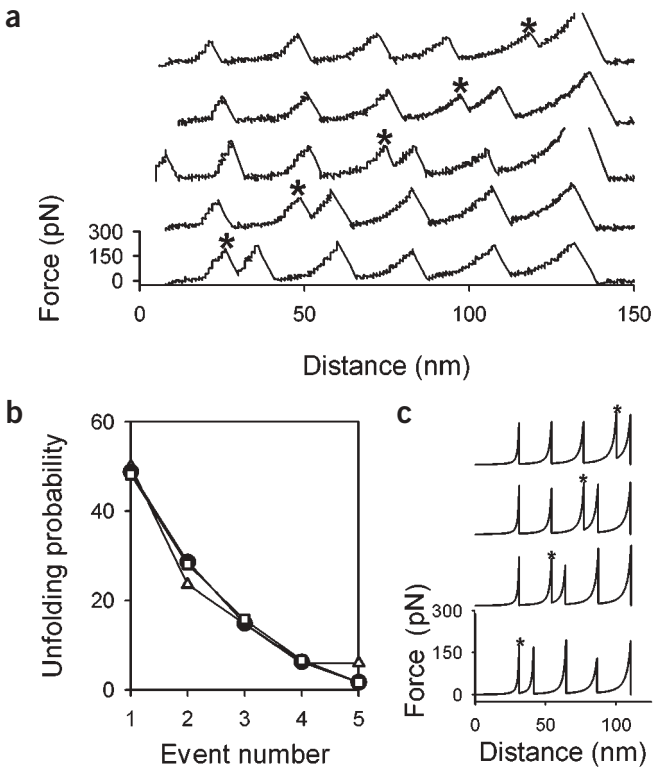

Figure 5 Force-extension profiles for $(I27)_4$E2lip3(+) can be used to obtain kinetic information. (**a**) Sample force-extension profiles of $(I27)_4$E2lip3(+). E2lip3(+) unfolding (*) occurs at any position in the unfolding sequence of the concatamer. After each E2lip3(+) unfolding event the force does not return to zero but to a point determined by the entropic restoring force of the unfolded polypeptide chain acting upon the cantilever. The smaller increase in chain length released upon E2lip3 unfolding relative to I27 (41 residues compared with 89 residues) results in a higher restoring force being applied on the system directly after this unfolding event and is well described by a WLC model of polymer elasticity (see **Fig. 2b**). (**b**) The probability of E2lip3(+) unfolding at each event number measured by experiment (△), estimated by fitting an analytical solution to the experimental unfolding probability at each event number (●) and Monte Carlo simulation (□). (**c**) Force-extension profiles for $(I27)_4$E2lip3(+) obtained by Monte Carlo simulation. The unfolding of E2lip3(+) is marked *.

events are visible for $(I27)_4$E2lip3(–) (**Fig. 2c**), each of which occurs with an unfolding distance, L_i, of 24.1 ± 0.2 nm (ΔL_c 27.1 ± 0.1 nm) and force of 187 ± 10 pN (700 nm s^{-1}) (**Fig. 3a–c**, bottom). These events represent the unfolding of the four I27 domains. Of the 190 unfolding peaks measured for this construct, only two events occurred with a distance substantially less than 24 nm (**Fig. 3a**, bottom). Each of the latter force-extension profiles contained five unfolding peaks, one occurring with a L_i ~ 10 nm. These traces presumably derive from a minor population of molecules that are lipoylated by virtue of trace amounts of lipoic acid in the bacterial growth medium (see Methods). Unfolding E2lip3(–) from its N and C termini would result in a ΔL_c of 24 nm, a distance considerably smaller than that for I27. No such events were observed here. This could be explained either by E2lip3(–) unfolding at a force that is no longer detectable using an AFM (<15 pN) or would result if the gold surface aberrantly destabilized or unfolded the E2lip3(–) domain. The latter explanation was considered improbable, because in both $(I27)_4$E2lip3(–) and $(I27)_4$E2lip3(+) the lipoyl domain is placed 12 Å from the surface (see Methods). Nonetheless, to obviate any effect of the gold surface, a fourth construct $(I27)_2$E2lip3(–)$(I27)_2$, was created in which the central I27 domain is replaced with E2lip3(–) (**Fig. 1a**). Force-extension profiles for this construct were essentially identical to those for $(I27)_4$E2lip3(–), in that all traces containing at least four I27 unfolding events (identified on the basis of the force (189 ± 4 pN at 700 nm s^{-1}), L_i (25.1 ± 0.3 nm) and L_c (27.9 ± 0.3 nm) showed no unfolding event for E2lip3 (**Fig. 2d**) but included a longer initial extension before the first unfolding event. This is consistent with E2lip3(–) unfolding at a very low force. The data clearly indicate that when subjected to a peeling force, the mechanical resistance of E2lip3 is reduced greatly relative to its mechanical resistance when subjected to a shearlike extension.

As a final confirmation of this interpretation, the total length of the unfolded concatamer (L_{cFinal}) in traces involving five ($(I27)_5$ and $(I27)_4$E2lip3(+)), or four ($(I27)_4$E2lip3(–) and $(I27)_2$E2lip3(–)$(I27)_2$) unfolding events was assessed by fitting a WLC model to the tip-polymer detachment peak of each force-extension profile. For $(I27)_5$, L_{cFinal} = 161.9 ± 1.2 nm, identical to the value of 161 nm expected for complete unfolding of all 473 residues in the concatamer. Similarly, L_{cFinal} for $(I27)_4$E2lip3(+) was found to be 144.3 ± 1.0 nm compared with an expected value of 145 nm, for the unfolding of four I27 domains, the linker regions and 41 residues of E2lip3. Finally, for $(I27)_4$E2lip3(–) and $(I27)_2$E2lip3(–)$(I27)_2$, L_{cFinal} was 157.4 ± 1.0 nm and 159.0 ± 2.5 nm, respectively, in agreement with expected values of 159 nm and 160 nm, assuming that four I27 domains, the linkers and 79 residues in E2lip3 unfold (these constructs differ in length by two residues). If E2lip3 did not unfold in $(I27)_4$E2lip3(–), L_{cFinal} would be 133 nm.

Given that the structure, hydrogen-bonding pattern, tertiary packing[11] and thermodynamic stability (see Methods) of E2lip3 are unaffected by lipoylation, these experiments demonstrate that the mechanical unfolding properties of E2lip3 are highly anisotropic. Thus, a single protein can show very different mechanical properties, depending on the direction of the applied force vector. This may reflect the position of secondary structural elements relative to the points of extension, consistent with analytical[17] and computational models[18], which predict that shearing and peeling of antiparallel β-strands result in very different mechanical responses. Similarly, the force at which chair-boat transitions occur in polysaccharides has been shown to depend on the type of glycosidic linkage found in the polymer[19,20].

Why do E2lip3(+) and E2lip3(–) unfold at different forces?

The manner in which force is applied to E2lip3(–) would clearly result in peeling of the N- and C-terminal strands from the rest of the structure. However, the way in which force is propagated through E2lip3(+) when extended by the N terminus and the lipoyl group attached to the side chain of Lys41 is less clear. MD simulations can be used to model the behavior of a protein under an external force[4,8] and, in conjunction with experimental data, have been used to describe the nature of an unfolding intermediate and the mechanical unfolding transition state for I27 (refs. 21,22). To picture the response of E2lip3 to an applied extension at different points, simulations of the unfolding behavior of E2lip3(+) and E2lip3(–) were carried out using a steered MD (SMD) approach at a range of pulling speeds (**Fig. 6a**,**b**). As expected, the magnitude of the unfolding force for E2lip3(+) decreases at slower pulling speeds, but the overall shape of the force profiles are unaffected over a 100-fold change of pulling speed. In accord with our experimental results, the MD simulations show that E2lip3(+) unfolds at a higher force than E2lip3(–) and displays a more marked force response to extension. By contrast, simulated unfolding of E2lip3(–)

© 2003 Nature Publishing Group http://www.nature.com/naturestructuralbiology

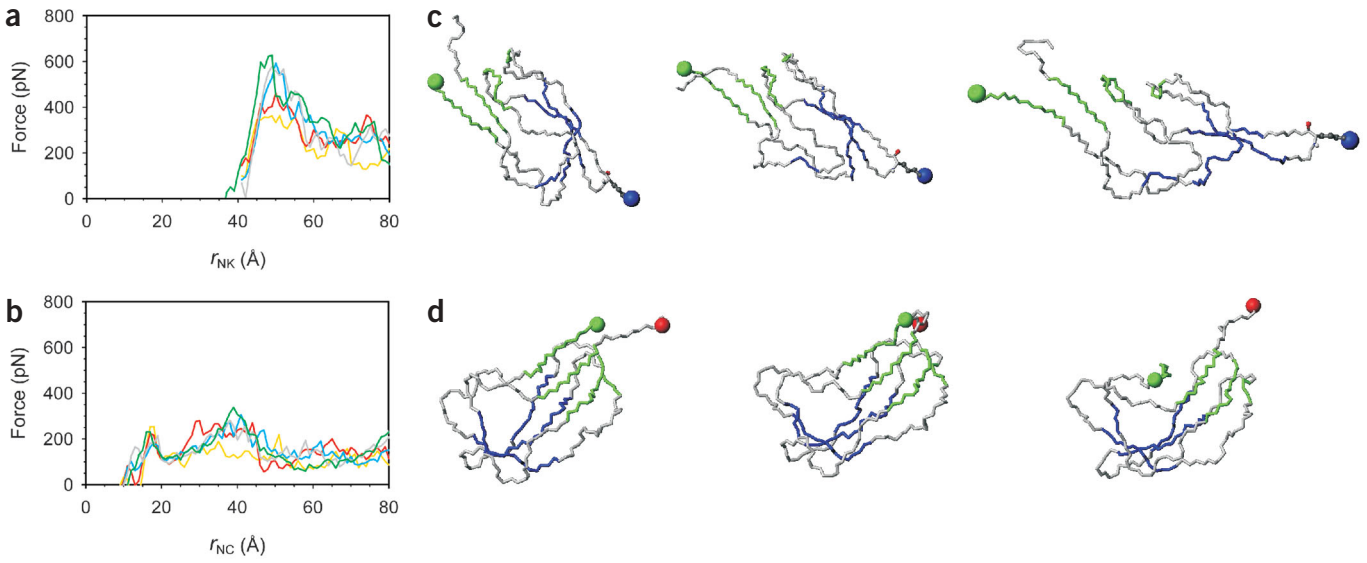

Figure 6 Force-extension profiles in a series of SMD simulations and structures at different time points. (**a**,**b**) Force-extension profiles for E2lip3(+) and E2lip(–), respectively, at 0.00125 Å ps^{-1} (orange), 0.01 Å ps^{-1} (red), 0.02 Å ps^{-1} (blue), 0.04 Å ps^{-1} (gray), 0.1 Å ps^{-1} (green) averaged over intervals of 1 Å in the extension and over four different trajectories for each pulling speed. The initial values for r_{NK} and r_{NC} (the distances between the N terminus and Lys41 and the N and C termini) are 40 Å and 9 Å for E2lip3(+) and E2lip3(–), respectively. (**c**,**d**) Sequence of events in simulated forced unfolding of E2lip3(+) and E2lip3(–), respectively. For clarity only the Cα backbone is shown. The side chain of Lys41 is also shown in **c**. Residues involved in elements of secondary structure in the native protein are shown in the same colors as **Figure 1**. Snapshots were taken every 10 ns (or at an increase in distance of 12.5 Å between the N terminus of the protein (green sphere) and either the Nζ atom of Lys41 (purple sphere in **c**) or the C terminus (red sphere in **d**). Snapshots are shown for 0, 10 and 20 ns.

showed trajectories with no obvious unfolding peaks. Instead, unfolding occurs gradually at low forces.

Snapshots of the unfolding process for E2lip3(+) and E2lip3(–) taken at different times during the unfolding simulation show that the mechanical unfolding pathways for these constructs differ substantially (**Fig. 6c**,**d**). Although details of the unfolding trajectories and the forces depend critically on the force fields used[23,24], the very different unfolding pathways for E2lip3(+) and E2lip(–) that are generated using the same force field confirm that E2lip3 unfolds at different forces and by different pathways when pulled in different defined directions. The response to force in a simulated system is thus highly anisotropic, in accord with our experimental observations.

DISCUSSION

It has been postulated that mechanical resistance may be determined by topology and is modulated by sequence effects[3–9]. Here we separated these effects by mechanically unfolding the same protein by pulling it in different directions. With one earlier exception, in which domains were concatenated by disulfide bonds[25], and the very recent results by the Fernandez group[26], all proteins studied to date have been unfolded by extension of their termini. This extension geometry results from the nature of the concatamerization process used to construct biomolecules suitable for such experiments[1,7,15,27–29]. This mode of extension is of functional relevance in naturally occurring modular proteins such as those from fibronectin[2], spectrin[29], tenascin[30] and titin[27]. However, technical requirements of this approach (such as immobilization via terminal cysteine residues) restrict the path through the mechanical unfolding landscape that can be explored by using these polymers.

The marked difference in the measured unfolding forces observed for E2lip3 immobilized in different ways demonstrates the importance of pulling geometry in defining the mechanical resistance of a protein. MD simulations on a small peptide[9] and an off-lattice model study[31] suggested that alteration of the points of extension can reveal different aspects of the energy landscape. The sensitivity of the mechanical response of E2lip3 to the applied pulling geometry indicates that the mechanical resistance of individual proteins cannot be described simply by consideration of chain sequence, structure, topology or kinetic stability, but will also depend on the geometry of the applied force vector. Manipulating the pulling geometry thus allows exploration of new features of a mechanical unfolding energy landscape. Control of the immobilization point, by varying the site of lipoylation, for example, could be used to map the mechanical unfolding landscape of proteins in great detail, especially when combined with MD simulations of the same process.

Pulling the same protein in different directions can result in very different mechanical phenotypes. Simulations[4] suggest that this anisotropy arises, at least in part, from the orientation of β-strands relative to the force vector, in accord with earlier results[3]. Theoretical predictions[17] and molecular models[18] based on simplified systems suggest that longitudinal shearing of *n* 'bonds' requires a breaking force equivalent to slightly less than *n* times the force required to rupture one such 'bond'. Modeling the longitudinal shearing of two $(Ala)_{10}$ antiparallel β-strands (containing ten interstrand hydrogen bonds) was found to occur at ~1,000 pN (ref. 18). By contrast, the application of force orthogonally to the β-strands (peeling) loads each hydrogen bond in turn, such that they fail consecutively at a lower force and pass the load to the next (modeling this process for $(Ala)_{10}$ resulted in unfolding at 40–120 pN)[18]. Scaling these results to the experimental value for $(I27)_4$E2lip3(+) (~175 pN) (to account for the rapid pulling rates used *in silico*) gives a value of 7–21 pN for E2lip3(–), in agreement with the experimental observations presented here.

Mechanically unfolding proteins using the AFM has demonstrated that (i) mechanical stability is not correlated with thermo-

© 2003 Nature Publishing Group http://www.nature.com/naturestructuralbiology

© 2003 Nature Publishing Group http://www.nature.com/naturestructuralbiology

dynamic stability[6,32] (ii) chemical and mechanical unfolding barriers are different[7,15] (iii) mechanical and chemical unfolding occur by different pathways[15,22] and (iv) mechanical resistance and the unfolding pathway depend upon the pulling geometry (this work and ref. 26). It is of note that similar observations have been made about the unfolding process *in vivo*. Some proteins must be unfolded to allow translocation into different cellular compartments[33] or degradation by the 26S proteasome[34] or ClpAP–XP[34] complexes. The rates of protein import or degradation of substrate proteins by these complexes do not correlate with the global thermodynamic or kinetic stability of the protein substrate[34,35]. Mutagenesis studies have shown that the same substrate protein is unfolded by different pathways when imported into mitochondria or unfolded chemically using denaturing agents[36]. Furthermore, experiments using circular permutants, proteins with different topologies or substrates in which the import or degradation 'tag' is placed at the N or C terminus, have shown that protein import and degradation rates are determined by the local structure of the polypeptide chain relative to the import or degradation 'tag'[34,36], respectively. Earlier work[6,7,15,22,32] and the anisotropy of the unfolding landscape, as shown here for E2lip3 and in ref. 26 for ubiquitin domains, accord with these observations and may help to explain how proteins that are thermodynamically, kinetically or apparently mechanically stable are unfolded *in vivo* at considerably lower forces than would be expected[37]. Parallel terminal β-strands that are directly hydrogen bonded are optimal for mechanical stability, whereas other arrangements of β-strands and/or α-helices at one of the chain termini result in proteins more responsive to force[3,34]. Rather than being a feature of the global properties of the polypeptide chain, the mechanical resistance of a protein domain can depend chiefly on which way it is pulled.

METHODS

Concatamer construction and purification. $(I27)_4$E2lip3(–) was constructed from (C47S C63S I27)$_5$ (ref. 12) by replacing the C-terminal domain with a PCR-generated cassette encoding E2lip3 (using pET11cE2p3 (ref. 10) as template) via a shuttle vector, as described[7]. This generates a concatamer that terminates $(I27)_4$LIEARALGG-E2lip3-CC and incorporates residues 2–80 of the published structure of E2lip3 (ref. 10). E2lip3 contains no cysteine residues. The only cysteines in the concatamer are at the C terminus and ensure specific immobilization to gold via these residues. Immobilization to gold thus places E2lip3 ~1.3 nm from the surface. $(I27)_4$E2lip3(+) was constructed in a similar fashion. This concatamer terminates $(I27)_4$LIEARALGG-E2lip3 and, for this construct, immobilization to gold via the lipoyl group places E2lip3 ~1.2 nm from the surface. The concatamer $(I27)_2$E2lip3(–)$(I27)_2$ contains an identical E2lip3 domain to those in $(I27)_4$E2lip3(+) and $(I27)_4$E2lip3(–) fused in frame to an I27 scaffold. The linker sequence in this case is $(I27)_2$LIEARGG-E2lip3-GGGLSSAR$(I27)_2$CC. This construct places E2lip3(–) ~10 nm from the surface. In all concatamers containing an E2lip3 domain, at least two glycine residues were included in the linker to this domain to minimize geometric and steric effects of the linkers.

All constructs were overexpressed and purified as described[7] except that 10 mg l^{-1} DL-6,8-thioctic acid (lipoic acid; Sigma) was included in the growth medium for $(I27)_4$E2lip3(+). Addition of this supplement results in 100% lipoylation, whereas no detectable modification occurs without supplementation of the medium[38]. This was confirmed using electrospray ionization mass spectrometry (ES-MS). All concatamers were purified to homogeneity using nickel chelate and gel filtration chromatography as described[7]. The molecular masses of the isolated proteins were assessed by ES-MS. Each construct gave a single species that was within error of the expected masses of 52,219, 50,938, 50,920 and 50,996 Da for $(I27)_5$, $(I27)_4$E2lip3(–), $(I27)_4$E2lip3(+) and $(I27)_2$E2lip3(–)$(I27)_2$, respectively.

Temperature and chemical equilibrium denaturation experiments monitored by circular dichroism spectroscopy on $(I27)_4$E2lip3(+) and $(I27)_4$E2lip3(–) confirmed that lipoylation has no effect on the thermodynamic stability of these constructs (data not shown).

Mechanical unfolding experiments and data analysis. Mechanical unfolding experiments were done and analyzed as described[7] at a protein concentration of ~1 μM and a tip retraction rate of 700 nm s^{-1}, unless otherwise stated. Only force-extension profiles with at least four unfolding events having the characteristic interpeak distance for the unfolding of an I27 domain (~25 ± 2 nm) were included in the data sets. The presence of four I27 peaks therefore ensures that the concatamer analyzed must have been attached to the cantilever via the N-terminal hexahistidine or $(His)_6$-$I27_1$ linker region in all heteropolymeric constructs.

Expected increases in contour length (ΔL_c) were estimated based on the number of structured residues released upon unfolding multiplied by the distance between two adjacent Cα atoms in a fully extended state (0.34 nm) (ref. 25) minus the initial distance between boundary structured residues.

Monte Carlo simulations of the mechanical unfolding process were carried out essentially as described[7,12] but modified to describe the unfolding of a heteropolymer: the parameters used for C47S C63S I27 were identical to those reported earlier (P = 0.4 nm, x_u = 0.29 nm, L_u = 28.0 nm, L_f = 4.0 nm and k_u^0 = 2.0 × 10^{-3} s^{-1}), and the parameters for E2lip3(+) were: P = 0.4 nm, x_u = 0.29 nm, L_u = 10.9 nm (obtained experimentally, see earlier), L_f = 3.3 nm and k_u^0 = 7.6 × 10^{-3} s^{-1}. Note: k_u^0 used for E2lip3(+) was the value estimated by probability arguments ($3.8k_u^0{}_{I27}$, see below). x_u for E2lip3(+) was determined to be 0.29 nm by Monte Carlo simulation of force versus log pulling speed data, obtained at pulling speeds of 100–2,500 nm s^{-1} (see **Fig. 4**).

Probability arguments were used to determine the fraction of the E2lip3(+) domains unfolding as the first, second to mth event in the pulling history. If a protein has L domains, one of which is unique, then there are L ways in which it can unfold, for example BAAAA, ABAAA, and so on, if the unique domain is B. The chance $\phi(m, L)$ of observing the unfolding of the unique protein as the mth event is given by

$$\phi(m,L) = \frac{R}{L}\prod_{i=1}^{m}\frac{L+1-i}{L+R-i}$$

where R is the ratio of the unfolding rate coefficient of the unique protein (E2lip3) to the others (C47S C63S I27)[12].

Molecular dynamics simulations. MD simulations were carried out using an all-atom model of the protein[39] and an implicit model for the solvent (EEF1)[40] that provides a potential-of-mean-force description of the solvent. Model 8 of the PDB file for E2lip3 (1QJO)[10] was chosen as the starting configuration as this structure is closest to the averaged structure of E2lip3 (0.8 and 1.2 Å r.m.s. deviation, Cα and all-atom, respectively). The SMD method[23] was used to mechanically unfold the protein: one atom is fixed and another is attached to a harmonic spring of spring constant 1,000 pN nm^{-1} and pulled away at constant speed (which varied between 1.25 × 10^8 and 1 × 10^{10} nm s^{-1}). Simulations were conducted by fixing the N terminus and pulling either the C terminus or the Nζ atom of Lys41. The protein was first equilibrated for 10 ns and a conformation selected every 1 ns as an initial conformation for SMD simulation. The Cα r.m.s. deviation during equilibration remained <3.5 Å. For each value of the pulling speed, four simulations were conducted, starting from different equilibrated conformations.

ACKNOWLEDGMENTS

We thank A. Berry for help with producing Figure 1 and K. Ainley for the large-scale microbial cultures. We thank A. Blake and the other members of the Radford laboratory for fruitful discussions. We acknowledge the Biotechnology and Biological Sciences Research Council, Engineering and Physical Sciences Research Council, University of Leeds, the Wellcome Trust and Forschungskredit der Universität Zürich for financial support. S.E.R. is a BBSRC Professorial Fellow. The manuscript is a contribution from the Astbury Centre for Structural Molecular Biology, which is part of the North of England Structural Biology Centre (NESBIC) and is funded by the BBSRC.

COMPETING INTERESTS STATEMENT

The authors declare that they have no competing financial interests.

Received 3 February; accepted 23 May 2003
Published online at http://www.nature.com/naturestructuralbiology/

1. Carrion-Vazquez, M. *et al.* Mechanical and chemical unfolding of a single protein: a comparison. *Proc. Natl. Acad. Sci. USA* **96**, 3694–3699 (1999).
2. Oberhauser, A.F., Badilla-Fernandez, C., Carrion-Vazquez, M. & Fernandez, J.M. The mechanical hierarchies of fibronectin observed with single-molecule AFM. *J. Mol. Biol.* **319**, 433–447 (2002).
3. Carrion-Vazquez, M. *et al.* Mechanical design of proteins—studied by single-molecule force spectroscopy and protein engineering. *Prog. Biophys. Mol. Biol.* **74**, 63–91 (2000).
4. Lu, H. & Schulten, K. Steered molecular dynamics simulations of force-induced protein domain unfolding. *Proteins* **35**, 453–463 (1999).
5. Klimov, D.K. & Thirumalai, D. Native topology determines force-induced unfolding pathways in globular proteins. *Proc. Natl. Acad. Sci. USA* **97**, 7254–7259 (2000).
6. Li, H.B., Oberhauser, A.F., Fowler, S.B., Clarke, J. & Fernandez, J.M. Atomic force microscopy reveals the mechanical design of a modular protein. *Proc. Natl. Acad. Sci. USA* **97**, 6527–6531 (2000).
7. Brockwell, D.J. *et al.* The effect of core destabilization on the mechanical resistance of I27. *Biophys. J.* **83**, 458–472 (2002).
8. Paci, E. & Karplus, M. Forced unfolding of fibronectin type 3 modules: an analysis by biased molecular dynamics simulations. *J. Mol. Biol.* **288**, 441–459 (1999).
9. Bryant, Z., Pande, V.S. & Rokhsar, D.S. Mechanical unfolding of a β-hairpin using molecular dynamics. *Biophys. J.* **78**, 584–589 (2000).
10. Jones, D.D., Stott, K.M., Howard, M.J. & Perham, R.N. Restricted motion of the lipoyl-lysine swinging arm in the pyruvate dehydrogenase complex of *Escherichia coli*. *Biochemistry* **39**, 8448–8459 (2000).
11. Perham, R.N. Swinging arms and swinging domains in multifunctional enzymes: catalytic machines for multistep reactions. *Annu. Rev. Biochem.* **69**, 961–1004 (2000).
12. Zinober, R.C. *et al.* Mechanically unfolding proteins: the effect of unfolding history and the supramolecular scaffold. *Protein Sci.* **11**, 2759–2765 (2002).
13. Grandbois, M., Beyer, M., Rief, M., Clausen-Schaumann, H. & Gaub, H.E. How strong is a covalent bond? *Science* **283**, 1727–1730 (1999).
14. Marko, J.F. & Siggia, E.D. Stretching DNA. *Macromolecules* **28**, 8759–8770 (1995).
15. Best, R.B., Li, B., Steward, A., Daggett, V. & Clarke, J. Can non-mechanical proteins withstand force? Stretching barnase by atomic force microscopy and molecular dynamics simulation. *Biophys. J.* **81**, 2344–2356 (2001).
16. Evans, E. & Ritchie, K. Dynamic strength of molecular adhesion bonds. *Biophys. J.* **72**, 1541–1555 (1997).
17. Williams, P.M. & Evans, E. In *Les Houches-Ecole d'Ete de Physique Theorique* Vol. 75, 187–203 (Springer, Heidelberg, Germany, 2002).
18. Rohs, R., Etchebest, C. & Lavery, R. Unraveling proteins: a molecular mechanics study. *Biophys. J.* **76**, 2760–2768 (1999).
19. Marszalek, P.E. *et al.* Atomic levers control pyranose ring conformations. *Proc. Natl. Acad. Sci. USA* **96**, 7894–7898 (1999).
20. Marszalek, P.E., Li, H.B., Oberhauser, A.F. & Fernandez, J.M. Chair-boat transitions in single polysaccharide molecules observed with force-ramp AFM. *Proc. Natl. Acad. Sci. USA* **99**, 4278–4283 (2002).
21. Marszalek, P.E. *et al.* Mechanical unfolding intermediates in titin modules. *Nature* **402**, 100–103 (1999).
22. Fowler, S.B. *et al.* Mechanical unfolding of a titin Ig domain: structure of unfolding intermediate revealed by combining AFM, molecular dynamics simulations, NMR and protein engineering. *J. Mol. Biol.* **322**, 841–849 (2002).
23. Lu, H., Isralewitz, B., Krammer, A., Vogel, V. & Schulten, K. Unfolding of titin immunoglobulin domains by steered molecular dynamics simulation. *Biophys. J.* **75**, 662–671 (1998).
24. Paci, E. & Karplus, M. Unfolding proteins by external forces and temperature: the importance of topology and energetics. *Proc. Natl. Acad. Sci. USA* **97**, 6521–6526 (2000).
25. Yang, G.L. *et al.* Solid-state synthesis and mechanical unfolding of polymers of T4 lysozyme. *Proc. Natl. Acad. Sci. USA* **97**, 139–144 (2000).
26. Carrion-Vazquez, M., Li, H., Marszalek, P.E., Oberhauser, A.F. & Fernandez, J.M. The mechanical stability of ubiquitin is linkage dependent. *Nat. Struct. Biol.* **10**, 738–743 (2003).
27. Rief, M., Gautel, M., Oesterhelt, F., Fernandez, J.M. & Gaub, H.E. Reversible unfolding of individual titin immunoglobulin domains by AFM. *Science* **276**, 1109–1112 (1997).
28. Carl, P., Kwok, C.H., Manderson, G., Speicher, D.W. & Discher, D.E. Forced unfolding modulated by disulfide bonds in the Ig domains of a cell adhesion molecule. *Proc. Natl. Acad. Sci. USA* **98**, 1565–1570 (2001).
29. Altmann, S.M. *et al.* Pathways and intermediates in forced unfolding of spectrin repeats. *Structure* **10**, 1085–1096 (2002).
30. Oberhauser, A.F., Marszalek, P.E., Erickson, H.P. & Fernandez, J.M. The molecular elasticity of the extracellular matrix protein tenascin. *Nature* **393**, 181–185 (1998).
31. Li, F.Y., Yuan, J.M. & Mou, C.Y. Mechanical unfolding and refolding of proteins: an off-lattice model study. *Phys. Rev. E* 6302, art. no.-021905 (2001).
32. Rief, M., Pascual, J., Saraste, M. & Gaub, H.E. Single molecule force spectroscopy of spectrin repeats: low unfolding forces in helix bundles. *J. Mol. Biol.* **286**, 553–561 (1999).
33. Neupert, W. & Brunner, M. The protein import motor of mitochondria. *Nat. Rev. Mol. Cell Biol.* **3**, 555–565 (2002).
34. Lee, C., Schwartz, M.P., Prakash, S., Iwakura, M. & Matouschek, A. ATP-dependent proteases degrade their substrates by processively unraveling them from the degradation signal. *Mol. Cell* **7**, 627–637 (2001).
35. Lim, J.H., Martin, F., Guiard, B., Pfanner, N. & Voos, W. The mitochondrial Hsp70-dependent import system actively unfolds preproteins and shortens the lag phase of translocation. *EMBO J.* **20**, 941–950 (2001).
36. Huang, S.H., Ratliff, K.S., Schwartz, M.P., Spenner, J.M. & Matouschek, A. Mitochondria unfold precursor proteins by unraveling them from their N-termini. *Nat. Struct. Biol.* **6**, 1132–1138 (1999).
37. Okamoto, K. *et al.* The protein import motor of mitochondria: a targeted molecular ratchet driving unfolding and translocation. *EMBO J.* **21**, 3659–3671 (2002).
38. Jones, D.D., Stott, K.M., Reche, P.A. & Perham, R.N. Recognition of the lipoyl domain is the ultimate determinant of substrate channelling in the pyruvate dehydrogenase multienzyme complex. *J. Mol. Biol.* **305**, 49–60 (2001).
39. Brooks, B.R. *et al.* Charmm—a program for macromolecular energy, minimization, and dynamics calculations. *J. Comput. Chem.* **4**, 187–217 (1983).
40. Lazaridis, T. & Karplus, M. Effective energy function for proteins in solution. *Proteins* **35**, 133–152 (1999).
41. Kraulis, P.J. MOLSCRIPT: a program to produce both detailed and schematic plots of protein structures. *J. Appl. Crystallogr.* **24**, 946–950 (1991).
42. Merritt, E.A. & Murphy, M.E.P. Raster3D Version 2.0—a program for photorealistic molecular graphics. *Acta Crystallogr. D* **50**, 869–873 (1994).
43. Kabsch, W. & Sander, C. Dictionary of protein secondary structure—pattern-recognition of hydrogen-bonded and geometrical features. *Biopolymers* **22**, 2577–2637 (1983).

© 2003 Nature Publishing Group http://www.nature.com/naturestructuralbiology

Corrigendum: Sequence elements outside the hammerhead ribozyme catalytic core enable intracellular activity

Anastasia Khvorova, Aurélie Lescoute, Eric Westhof & Sumedha D Jayasena
Nat. Struct. Biol. **10,** 708–712 (2003).

Figure 4e in this paper contained mistakes. The labels for the fourth, fifth and sixth sets of data should be sTRSV + PL1, sTRSV + PL2 and sTRSV + PL1&2, respectively. We apologize for the inconvenience this may have caused.

Erratum: Pulling geometry defines the mechanical resistance of a β-sheet protein

David J Brockwell, Emanuele Paci, Rebecca C Zinober, Godfrey S Beddard, Peter D Olmsted, D Alastair Smith, Richard N Perham & Sheena E Radford
Nat. Struct. Biol. **10,** 731–737 (2003).

A mistake was introduced during production of this paper. This mistake was on page 731, line 4 of the second paragraph in the 'Results' section. The correct sentence should read: "The parent $(I27)_5$ homopolymer has been described and is composed of five copies of a mutated C47S C63S domain[7,12]." We apologize for any inconvenience this may have caused.

© 2003 Nature Publishing Group http://www.nature.com/naturestructuralbiology